

Carbon Stock Mapping in Urban Areas Based on Vegetation Index Comparison from Sentinel-2A Imagery

Sunaryo, D. K.,^{1*} Suhari, K. T.,¹ Dubu, V. M. N.¹ and Caecarma, G. A. A.²

¹Department of Geodetic Engineering, Faculty of Civil Engineering & Planning, Institut Teknologi Nasional Malang, Indonesia

²Department of Civil Engineering, Faculty of Engineering, Universitas Brawijaya, Indonesia

E-mail: dekaitn@gmail.com

*Corresponding Author

DOI: <https://doi.org/10.52939/ijg.v22i2.4793>

Abstract

This study investigates the spatial distribution of urban vegetation carbon stocks by comparing multiple vegetation index algorithms derived from Sentinel-2A satellite imagery. Urban carbon stock serves as a critical indicator of environmental sustainability, reflecting land cover characteristics and vegetation quality. The research workflow included radiometric correction, calculation of four vegetation indices: NDVI, EVI, ARVI, and SAVI conversion of index values into biomass estimates, and subsequent carbon stock computation using established allometric equations. Field-based measurements were used for validation. The results showed strong positive correlations between all vegetation indices and field-observed biomass ($R^2 > 0.90$). Among them, NDVI demonstrated the highest predictive accuracy ($R^2 = 0.91$), while EVI, ARVI, and SAVI tended to slightly underestimate biomass in areas with dense canopy cover or sparse vegetation. Spatial mapping of NDVI-derived carbon stocks revealed significant heterogeneity across sub-districts, with values ranging from below 600 tons/ha in densely built-up zones to over 900 tons/ha in peri-urban green areas. The total estimated carbon stock in Malang City was 3,861.35 tons/ha, with the highest concentrations identified in urban parks, forested areas, and historical green corridors. Overall, NDVI proved to be the most reliable index for urban carbon stock estimation using Sentinel-2A data. These findings highlight the necessity of preserving high-carbon zones, enhancing ecological buffer regions, and implementing targeted urban greening initiatives to support climate change mitigation and sustainable city planning.

Keywords: Biomass Estimation, NDVI, Sentinel-2A Imagery, Urban Carbon Stock, Urban Sustainability

1. Introduction

Climate change and global warming have accelerated in recent decades, largely driven by the increasing concentration of greenhouse gases (GHGs) in the atmosphere [1]. Among various GHGs, carbon dioxide (CO₂) is the dominant contributor to global warming and shifts in climate patterns. Urban areas are recognized as major sources of CO₂ emissions, primarily originating from transportation, industry, energy consumption, food production, and waste management. Rapid urban expansion is often accompanied by land-use change, particularly the conversion of vegetated and permeable areas such as urban forests, agricultural land, and green open spaces into built-up areas for residential, commercial, and industrial purposes. These land use/land cover (LULC) changes directly reduce the capacity of ecosystems to sequester atmospheric carbon, thereby lowering the total urban carbon stock.

Carbon stock is defined as the amount of carbon stored in vegetation biomass and soils, which plays a crucial role in climate change mitigation and sustainable urban development [2]. Higher vegetation density and biomass correspond to greater carbon sequestration potential; conversely, the loss of vegetation due to land conversion reduces carbon uptake capacity and increases net CO₂ emissions. In response, many countries and international organizations have emphasized the integration of green infrastructure into urban spatial planning. Such policies aim to preserve or enhance green open spaces including urban forests, parks, and green belts to improve environmental quality, strengthen carbon sequestration capacity, and support climate mitigation strategies such as carbon trading and emission reduction [3] and [4].

For this reason, industrial and residential zones are often required to allocate space for urban forests or green belts as a means to maintain carbon sinks and ecological services.

Monitoring carbon stocks in urban areas requires accurate, efficient, and large-scale methods. Conventional biomass surveys are time- and cost-intensive, with limited spatial coverage. By contrast, satellite remote sensing provides an effective alternative for multi-temporal and multi-spatial monitoring of vegetation conditions. One widely used approach is the application of vegetation indices derived from multispectral imagery, such as that captured by Sentinel-2A. Vegetation indices are mathematical transformations of spectral reflectance values designed to highlight vegetation properties. Commonly used indices include the Normalized Difference Vegetation Index (NDVI), Atmospherically Resistant Vegetation Index (ARVI), Enhanced Vegetation Index (EVI), and Soil Adjusted Vegetation Index (SAVI) [5] and [6]. NDVI is widely applied due to its simplicity and sensitivity to chlorophyll content; ARVI reduces the influence of atmospheric scattering; EVI minimizes background soil effects and saturation in high-biomass areas; and SAVI compensates for soil brightness, making it suitable for sparsely vegetated regions [7] and [8].

Previous studies have shown a strong relationship between vegetation index values and aboveground biomass estimates, enabling indirect estimation of carbon stocks [9]. However, most research has focused on a single index, with limited comparative evaluations of multiple indices simultaneously, particularly in tropical urban environments. Furthermore, few studies have assessed the accuracy of different indices in estimating urban carbon stocks in Indonesian cities, including Malang, which has undergone rapid LULC transformation.

Malang City, located in East Java Province, is one of the fastest-growing cities in Indonesia in terms of both population and spatial development [10]. The conversion of agricultural land, green open spaces, and peri-urban vegetation into built-up areas has significantly altered the dynamics of urban carbon storage. This condition necessitates comprehensive spatial analysis to measure vegetation loss and its impacts on urban carbon reserves.

This study focuses on analysing the relationship between vegetation indices (NDVI, ARVI, EVI, and SAVI) and aboveground biomass estimation for calculating carbon stocks, comparing the accuracy of these indices in estimating urban carbon stocks, and examining the spatial distribution of carbon stocks in Malang City using Sentinel-2A imagery. Given the rapid pace of climate change and land conversion in urban areas, a comprehensive evaluation of

vegetation indices for carbon stock modelling in tropical cities is urgently needed. The key contribution of this study lies in providing a quantitative assessment of NDVI, ARVI, EVI, and SAVI for estimating carbon stocks in Malang City, Indonesia. The findings are expected to support urban green infrastructure planning, climate change mitigation strategies, and national greenhouse gas reduction targets at the city level.

2. Methods

2.1 Study Site

The study was conducted in Malang City, East Java Province, Indonesia. Malang is located in a highland region with elevations ranging from 440 to 667 meters above sea level. Astronomically, the city lies between 112.06°–112.07° E longitude and 7.06°–8.02° S latitude. The topography of Malang is predominantly hilly and surrounded by upland areas. Administratively, the city is bordered to the north by Singosari and Karangploso Sub-districts (Malang Regency), to the east by Pakis and Tumpang Sub-districts (Malang Regency), to the south by Tajinan and Pakisaji Sub-districts (Malang Regency), and to the west by Wagir and Dau Sub-districts (Malang Regency). Based on these geographical characteristics, Malang City represents a rapidly developing urban area in a highland setting, characterized by a relatively cool climate and higher population density compared to the surrounding regions. The study area is illustrated in Figure 1. In principle, the methodology of this study consists of processing Sentinel-2A imagery and conducting regression analyses to examine the relationship between vegetation index values (NDVI, ARVI, EVI, and SAVI) and aboveground biomass estimation used in carbon stock calculations. The analysis also includes a comparative assessment of the accuracy of each vegetation index in estimating urban carbon stocks, as well as spatial mapping of carbon stock distribution across the city area based on the calculated vegetation indices. The overall workflow of the research methodology is presented in Figure 2.

2.2 Image Processing

A wide range of satellites record Earth's surface conditions, among which Sentinel-2A plays a prominent role. The Sentinel-2A satellite is equipped with the MultiSpectral Instrument (MSI), which captures high-resolution multispectral data for various environmental monitoring applications. In this study, imagery acquired by the MSI sensor was utilized to calculate several vegetation indices, namely NDVI, ARVI, EVI, and SAVI, which were subsequently applied to estimate aboveground biomass as the basis for carbon stock calculation.

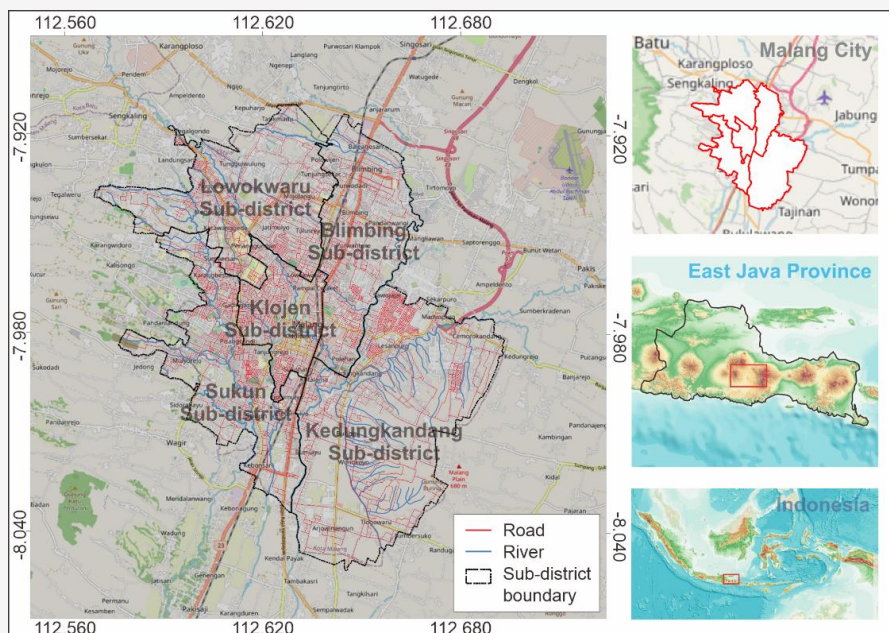


Figure 1: Malang City, East Java, Indonesia

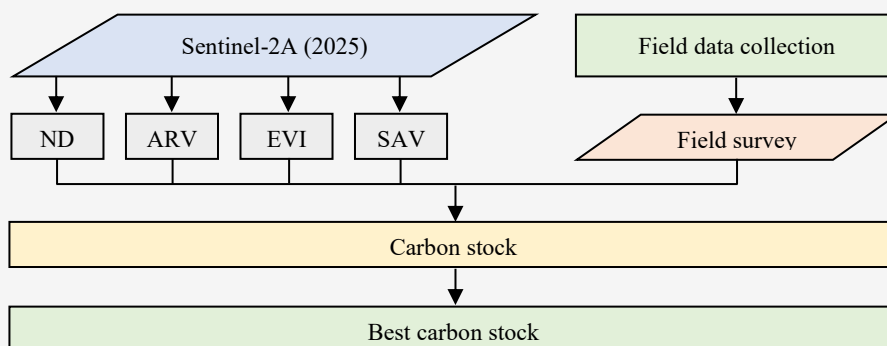


Figure 2: Carbon stock estimation methodology

These vegetation indices reflect the level of vegetation greenness in urban areas and thus serve as indicators of land use/land cover (LULC) changes that influence carbon storage. Image processing was carried out using Geographic Information System (GIS) software to generate spatially explicit maps of carbon stock distribution in Malang City.

2.3 NDVI

The Normalized Difference Vegetation Index (NDVI) is one of the primary indicators used to measure vegetation density as shown in Table 1. This index plays an essential role in detecting vegetation cover, assessing vegetation density, and monitoring plant health dynamics. NDVI values are influenced by land cover characteristics, including the presence, density, and specific attributes of different vegetation types. In addition, NDVI effectively represents the photosynthetic capacity of vegetation covering the land surface. Technically, NDVI is calculated

through a mathematical combination of red and near-infrared (NIR) spectral reflectance, which has long been utilized as a reliable indicator of vegetation presence and condition. The NDVI calculation, as defined in Equation 1, is performed using the near-infrared (NIR) and red reflectance values derived from vegetation.

$$NDVI = \frac{NIR - RED}{NIR + RED} \quad \text{Equation 1}$$

Where:

NDVI = Normalized Difference Vegetation Index
NIR = Band Near Infra-Red
RED = Band Red

Based on the Regulation of the Minister of Forestry of the Republic of Indonesia No. P.12/Menhut-II/2012, which constitutes the second amendment to

Regulation No. P.32/Menhut-II/2009 concerning the procedures for preparing the Technical Plan for Forest and Land Rehabilitation in Watershed Areas (RTK RHL-DAS), NDVI values are classified into five main categories [11].

Table 1: Vegetation density classification

Class	NDVI Range	Description
1	-1 to -0.03	Non-vegetated land
2	-0.03 to 0.15	Very low density
3	0.15 to 0.25	Low density
4	0.26 to 0.35	Moderate density
5	0.36 to 1.00	High density

2.4 ARVI

The Atmospherically Resistant Vegetation Index (ARVI) is a vegetation index specifically designed to reduce sensitivity to atmospheric effects, particularly aerosols. Modification of the Normalized Difference Vegetation Index (NDVI) to correct atmospheric scattering effects in the red reflectance spectrum by incorporating information from the blue wavelength. Compared to other vegetation indices, the ARVI, defined in Equation 2, demonstrates greater resistance to topographic influences, making it particularly effective for monitoring vegetation in tropical mountainous regions that are frequently exposed to soot resulting from logging and land-clearing activities.

$$ARVI = \frac{NIR - [RED - \gamma(BLUE - RED)]}{NIR + [RED - \gamma(BLUE - RED)]}$$

Equation 2

Where:

γ = Gamma coefficient with a value of 1
 $BLUE$ = Blue spectral reflectance

2.5 EVI

The Enhanced Vegetation Index (EVI) was developed to improve the performance of the Normalized Difference Vegetation Index (NDVI) by enhancing the vegetation signal in areas with a high Leaf Area Index (LAI). This index utilizes blue spectral reflectance to correct for soil background effects and reduce atmospheric influences, including aerosol scattering. EVI is particularly effective in regions with dense vegetation cover, where NDVI tends to saturate. Generally, EVI values for vegetation pixels range from 0 to 1; however, the presence of bright elements such as clouds or white-painted buildings, as well as dark features such as water bodies, may generate anomalous pixel values in EVI imagery. Moreover, the EVI, defined in Equation 3, is widely used to analyze variations in

vegetation growth across both densely and sparsely vegetated areas.

$$EVI = G \frac{NIR - RED}{L + NIR - C_1 RED - C_2 BLUE}$$

Equation 3

Where:

G = Gain factor (set to 2.5, with EVI values ranging from -1 to 1)
 L = Canopy and soil background adjustment factor (set to 1)
 C_1 = Aerosol resistance coefficient with a value of 6
 C_2 = Aerosol resistance coefficient with a value of 7.5

2.6 SAVI

The Soil Adjusted Vegetation Index (SAVI) was developed to minimize the influence of soil brightness on vegetation measurements. Incorporated a soil adjustment factor (L) into the NDVI calculation to correct for disturbances caused by variations in soil colour, moisture, and characteristics. Unlike NDVI, which is more general, SAVI is specifically designed to account for the contribution of soil reflectance within image pixels. The factor L functions as a canopy background adjustment, and its value depends on vegetation density. Recommended using $L=0.5$ as the optimal parameter to accommodate first-order variations in soil background. This method is particularly effective in sparsely vegetated areas, where the soil surface remains visible through canopy gaps [12]. The SAVI is defined in Equation 4.

$$SAVI = \frac{1.5(NIR - RED)}{NIR + RED + L}$$

Equation 4

Where:

L = Soil adjustment factor with a value of 0.5

2.7 Field Survey Measurements

Field data collection was conducted to provide the empirical basis for estimating vegetation biomass and carbon stock in the study area. The field survey followed standardized procedures in accordance with the Indonesian National Standard (SNI 7724:2011) on Measurement and Calculation of Carbon Stock: Field Measurement for Land-Based Carbon Accounting [13]. This ensured the scientific reliability, reproducibility, and comparability of the collected data. The sampling strategy employed a systematic random sampling approach, ensuring adequate spatial representation of different

vegetation structures across the administrative boundary of Malang City. The minimum number of sample plots was determined using the Equation 5.

$$A = TSM + \frac{L}{1,500}$$

Equation 5

Where:

- A = total number of required samples
- TSM = 50 (base sample size)
- L = total land area in hectares

Based on this formula, a minimum of 57 sample plots was established across the Malang city with the area of 11,006 ha. The spatial distribution of these plots was stratified according to vegetation density derived from Sentinel-2A NDVI classification, ensuring coverage of both dense and sparse canopy zones. Each plot was georeferenced using the Timestamp Camera application, which recorded tree locations with embedded GPS coordinates and photographic documentation. The coordinates were later cross-validated and visualized within QGIS, ensuring spatial consistency with the administrative boundary shapefile of Malang City.

The implementation of this research required various field and supporting equipment. The main instruments included a laptop for data processing, a phi band (diameter tape) for measuring tree diameters, as well as measuring tapes and rulers for distance measurement. In addition, wooden stakes were used as plot boundary markers, along with a roll meter, raffia string for marking, and a smartphone equipped with supporting applications. Writing materials and measurement sheets were also utilized for recording field data.

Field data collection was carried out through several stages. Tree coordinate data were obtained using the Timestamp Camera application installed on a smartphone, which allows for the simultaneous recording of geographic coordinates and visual documentation. The determination of sample plots was adjusted according to tree diameter: plots of 20 × 50 m were established for trees with a diameter greater than 30 cm, while plots of 20 × 20 m were used for trees with a diameter of less than 30 cm. Within each plot, all trees meeting the diameter criteria were measured. The average number of trees per plot ranged from 12–25, depending on stand density. For each tree, species identification, DBH, and geographic coordinates were recorded. A total of 1,215 individual trees were measured across all plots.

The phi band, or diameter tape, is a measuring instrument designed to determine both the circumference and diameter of tree stems. This tool

is commonly made of cloth, steel, or plastic, with a width of approximately 12 mm. The principle of diameter measurement using a phi band is based on the assumption that the tree cross-section is a perfect circle. The diameter (D) is calculated from the stem circumference (K) using the formula $K = \pi \times D$, where π is equal to 22/7 or 3.14. The use of a phi band offers several advantages, including its lightweight and portable design, relatively low cost, adequate accuracy, and applicability for measuring both wet and dirty wood surfaces. Moreover, the measurement process is practical, requiring only a single encirclement of the tree stem [14]. All field coordinates and calculated carbon stock values were imported into QGIS in CSV format and projected under EPSG:32749 – WGS 84/UTM Zone 49S. These georeferenced points served as ground-truth data for regression analysis against satellite-derived vegetation indices. The consistency between spatial data layers was validated through overlay inspection and coordinate matching, ensuring the robustness of spatial correlation analysis.

The combination of systematic sampling, adequate sample size, and standardized measurement protocol enhances the scientific credibility of this study. The inclusion of detailed spatial and biometric data ensures that carbon stock estimates are statistically reliable, spatially representative, and reproducible for similar urban ecosystem assessments.

2.8 Carbon Stock Estimations

The calculation of total forest carbon stock was carried out through field measurements, including the measurement of Diameter at Breast Height (DBH) in each sample plot. This study focused only on above-ground biomass (AGB), while below-ground biomass was not considered. Biomass estimation was performed using the following allometric in Equation 6.

$$\ln(TAGB) = -1,201 + 2,196\ln(DBH)$$

Equation 6

Where:

- $TAGB$ = Above-ground biomass in kilograms (kg)
- DBH = Tree diameter at breast height (1.3 m above the ground surface) in centimetres (cm)

This equation represents a non-linear relationship between Total Above-Ground Biomass ($TAGB$) and DBH . To obtain $TAGB$ values directly, the equation was transformed into its exponential form, as follows in Equation 7.

$$TAGB = e^{-1.201} DBH^{2.196} \quad \text{Equation 7}$$

The estimated biomass values were then used to calculate the carbon stock stored in vegetation. Approximately 47% of biomass consists of carbon. Thus, the carbon stock (C) was estimated by multiplying biomass (B) by a conversion factor of 0.47, expressed in the following Equation 8 [15].

$$C = 0.47B \quad \text{Equation 8}$$

Where:

C = Carbon stock (kg/tree)

B = Biomass (kg)

The relationship between remote sensing data and biomass was further analysed using exponential regression. In this analysis, remote sensing data served as independent variables, while field biomass acted as the dependent variable. The remote sensing dataset included digital numbers (DN) from single spectral bands (red, green, blue, and near-infrared) as well as various vegetation indices such as NDVI, EVI, SAVI, and ARVI. Each parameter was correlated with field-measured biomass to determine the highest correlation coefficient (greater than 0.5), which indicates the effectiveness of the model in estimating biomass and carbon stock. The exponential regression equation for biomass is expressed as follows in Equation 9.

$$B = aX^b \quad \text{Equation 9}$$

Where:

B = Biomass (expressed in kg, tons, or Mg/ha)

X = Predictor variable (e.g., tree diameter)

a and b = Regression coefficients obtained from statistical analysis

3. Result and Discussion

The satellite imagery used in this study was obtained from Sentinel-2A, recorded in 2025, covering the administrative area of Malang City as illustrated in Figure 3. All imagery was downloaded through the USGS Earth Explorer (or the Copernicus Open Access Hub when using Sentinel's official source). Image selection was conducted by considering cloud coverage, where only scenes with less than 10% cloud cover were used to ensure optimal data quality. The selected imagery was subsequently processed using QGIS software to extract the spatial and spectral parameters required for this study.

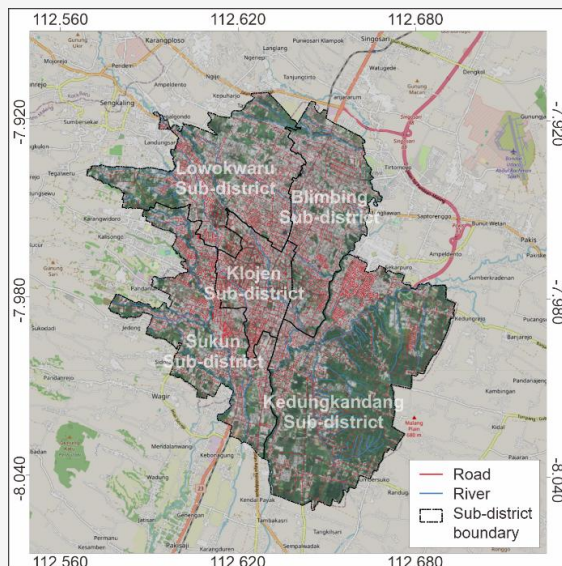


Figure 3: Sentinel-2A of Malang City, East Java, Indonesia

3.1 Relationship between Field-Based NDVI and Remotely Sensed NDVI Biomass

The calculation of NDVI across the entire study area was conducted using Equation (1). The analysis results revealed variations in NDVI values within a certain range, where positive values dominated in most areas covered by vegetation, while negative values were observed in non-vegetated areas such as dense settlements, open lands, and other built-up zones. These findings indicate differences in vegetation density, which can serve as a basis for biomass and carbon stock estimation in urban areas. The 2025 NDVI distribution of Malang City is presented in Figure 4.

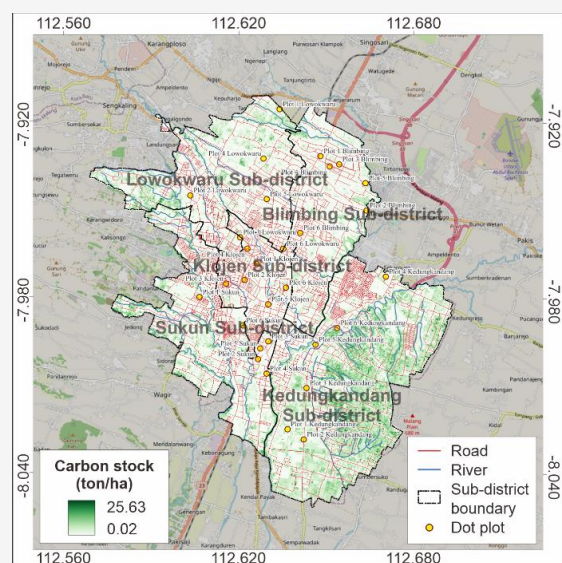


Figure 4: NDVI of Malang City (2025)

The relationship between field-based NDVI and remotely sensed NDVI-derived biomass was analysed to evaluate the accuracy of vegetation indices generated from Sentinel-2A imagery in estimating urban carbon stocks. Field-based NDVI values were obtained through direct measurements of vegetation reflectance using standardized field procedures, while above-ground biomass was calculated based on tree diameter measurements (Diameter at Breast Height/DBH) and the application of allometric equations.

Figures 5 and 6 illustrate the relationship between NDVI and biomass from both field measurements and remote sensing data. In parallel, remotely sensed NDVI values were extracted from atmospherically corrected Sentinel-2A imagery using the red and near-infrared bands. A comparative statistical correlation analysis between the two datasets was conducted to assess the strength of association and the reliability of satellite-derived NDVI in representing actual vegetation biomass. A strong positive correlation between field-based and remotely sensed NDVI confirms that Sentinel-2A imagery is an effective tool for monitoring urban vegetation conditions and estimating carbon stock. This approach supports the integration of remote sensing and field measurements for comprehensive urban carbon stock mapping.

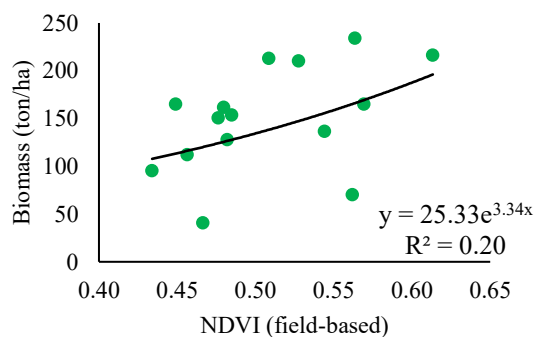


Figure 5: NDVI and biomass relationship (field-based)

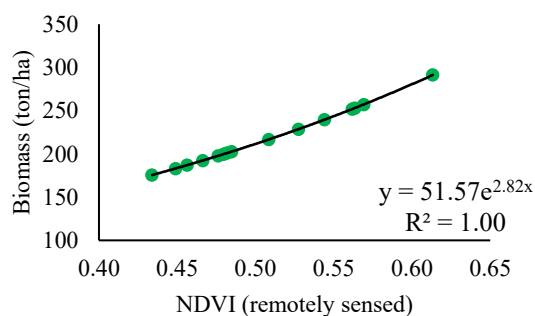


Figure 6: NDVI and biomass relationship (remotely sensed)

The coefficient of variation between field-based NDVI and remotely sensed NDVI was further compared with biomass (ton/ha). The relationship between NDVI (field-based and remotely sensed) and biomass is presented in Figure 7.

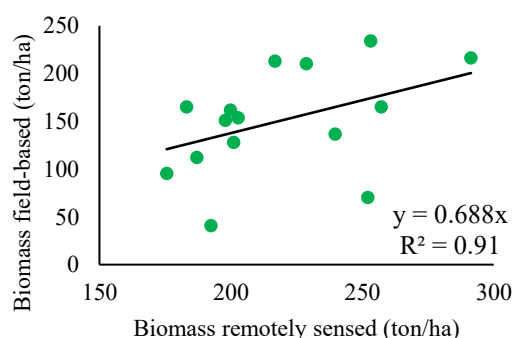


Figure 7: Field-based NDVI and remotely sensed NDVI biomass

The linear regression analysis between field-measured biomass and biomass estimated from Sentinel-2A imagery demonstrated a very strong relationship, with a coefficient of determination (R^2) of 0.91. This result indicates that 91% of the variation in field biomass can be explained by remotely sensed biomass estimation. The regression equation obtained was $y = 0.6884x$, suggesting that, in general, biomass values estimated from satellite data tend to be higher than those from field measurements, particularly in areas with dense vegetation cover.

3.2 Relationship between Field-Based ARVI and Remotely Sensed ARVI Biomass

The Atmospherically Resistant Vegetation Index (ARVI) was computed using Equation (2). The analysis revealed positive values in vegetated areas, whereas low to negative values were predominantly associated with non-vegetated surfaces. Compared with NDVI, ARVI is less affected by atmospheric distortions, thereby providing a more robust representation of vegetation conditions. The spatial distribution of ARVI in Malang City for 2025 is presented in Figure 8.

ARVI utilizes the blue, red, and near-infrared bands of Sentinel-2A, which enhances its resilience against atmospheric variability. Comparative analysis between field-based ARVI and satellite-derived ARVI demonstrated a strong positive correlation with above-ground biomass (ton/ha). Although the correlation strength was comparable to NDVI, ARVI exhibited greater stability under heterogeneous atmospheric conditions. This finding highlights ARVI as a reliable alternative for urban carbon stock estimation when integrating ground-

based observations with remote sensing data. The relationships between ARVI and biomass are illustrated in Figures 9 and 10.

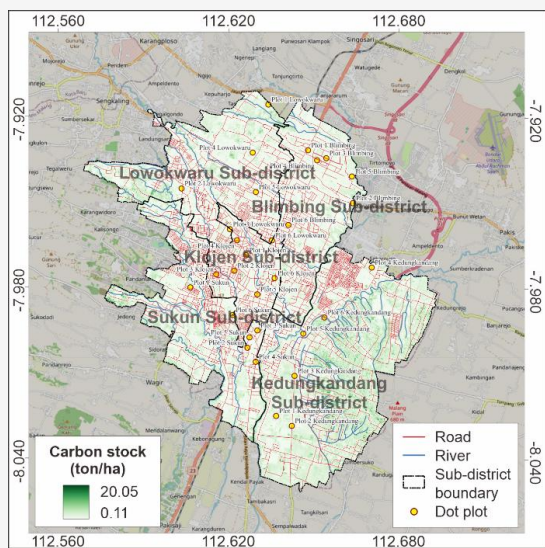


Figure 8: ARVI of Malang City (2025)

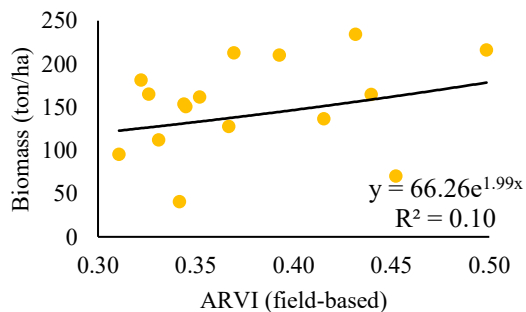


Figure 9: Relationship between field-based ARVI and biomass

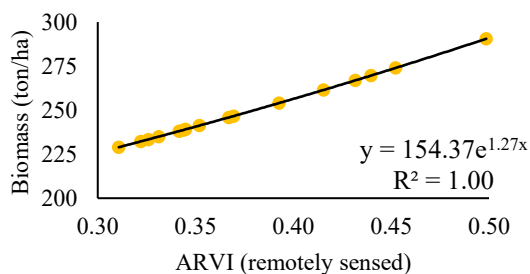


Figure 10: Relationship between remotely sensed ARVI and biomass

Additionally, the relationship field-based and remotely sensed ARVI biomass (ton/ha) is illustrated in Figure 11. Linear regression analysis yielded a

coefficient of determination (R^2) of 0.90, indicating that 90% of the variation in field-measured biomass could be explained by satellite-derived ARVI estimates. This robust statistical relationship underscores the effectiveness of ARVI as a vegetation index for quantifying above-ground biomass and carbon stocks in urban ecosystems.

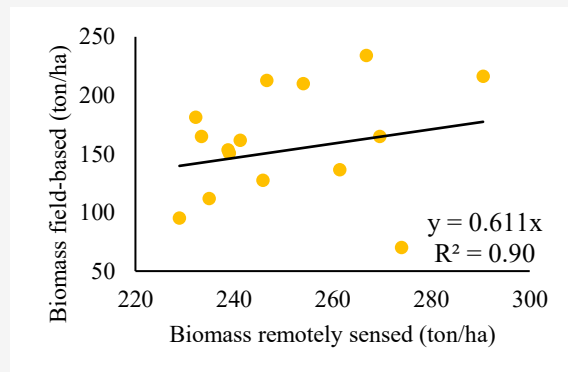


Figure 11: Field-based ARVI and remotely sensed ARVI biomass

3.3 Relationship between Field-Based EVI and Remotely Sensed EVI Biomass

The Enhanced Vegetation Index (EVI) was calculated using Equation (3). The results showed high values in areas with dense vegetation and low values in non-vegetated surfaces. Compared with NDVI, EVI is more sensitive to variations in high canopy density and is less influenced by atmospheric distortions and soil background effects. The spatial distribution of EVI in Malang City for 2025 is presented in Figure 12.

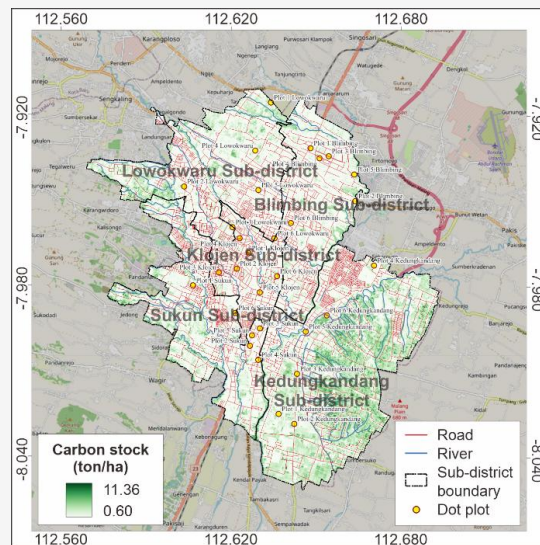


Figure 12: EVI of Malang City (2025)

EVI was analysed to address the limitations of NDVI, particularly its saturation in densely vegetated regions. By incorporating the blue, red, and near-infrared bands of Sentinel-2A, EVI reduces soil background interference and minimizes atmospheric effects, including aerosol scattering. Comparative analysis between field-based and satellite-derived EVI demonstrated a strong positive correlation with above-ground biomass (ton/ha). Notably, EVI outperformed NDVI and ARVI in areas of dense vegetation, underscoring its effectiveness in urban carbon stock estimation when integrating ground-based and remote sensing observations. The relationships between EVI and biomass are illustrated in Figures 13 and 14.

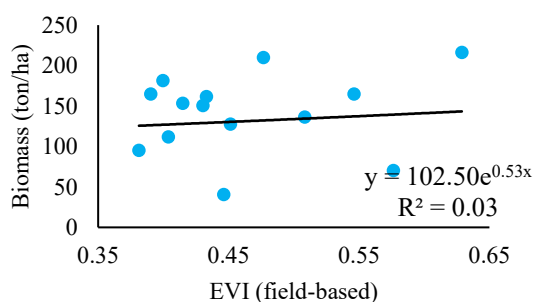


Figure 13: Relationship between field-based EVI and biomass

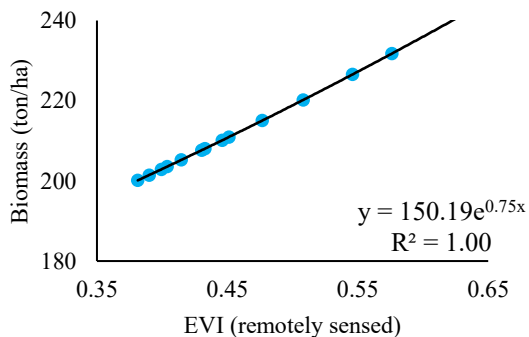


Figure 14: Relationship between remotely sensed EVI and biomass

Furthermore, the relationship between field-based and remotely sensed EVI with biomass (ton/ha) is presented in Figure 15. Linear regression analysis yielded a coefficient of determination (R^2) of 0.90, indicating that 90% of the variation in field-measured biomass could be explained by satellite-derived EVI estimates. This robust performance demonstrates that EVI provides a reliable and scalable approach for quantifying above-ground biomass and carbon stocks in urban ecosystems.

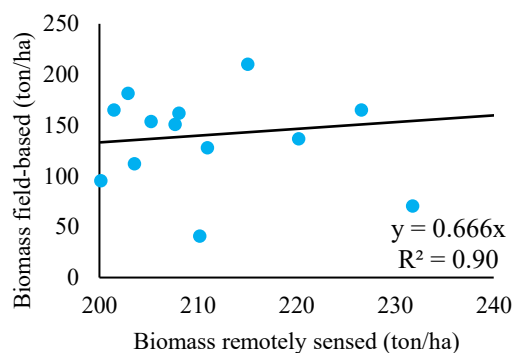


Figure 15: Field-based EVI and remotely sensed EVI biomass

3.4 Relationship between Field-Based SAVI and Remotely Sensed SAVI Biomass

The Soil Adjusted Vegetation Index (SAVI) was analysed to mitigate the influence of soil background, which often reduces the accuracy of vegetation indices, particularly in urban areas with low to medium canopy density. By incorporating the red and near-infrared bands of Sentinel-2A along with a soil adjustment factor (L), SAVI provides more stable biomass estimates compared to NDVI. The spatial distribution of SAVI in Malang City for 2025 is presented in Figure 16

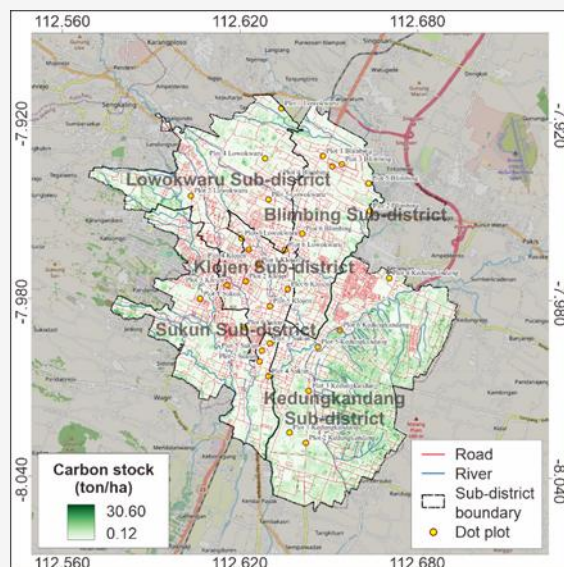


Figure 16: SAVI of Malang City (2025)

Comparative analysis between field-based and satellite-derived SAVI revealed a strong positive correlation with above-ground biomass (ton/ha), with superior performance in areas characterized by sparse vegetation cover. In contrast, NDVI is more reliable in densely vegetated regions but is biased in

open soil conditions, EVI is more sensitive to high canopy variability, and ARVI performs better under variable atmospheric conditions due to its resistance to aerosol effects. SAVI, therefore, plays a critical role in balancing the limitations of NDVI in mixed urban landscapes, making it highly relevant for urban carbon stock mapping. The relationships between SAVI and biomass are illustrated in Figures 17, 18, and 19. Furthermore, the relationship between field-based and remotely sensed EVI with biomass (ton/ha) is presented in Figure 15.

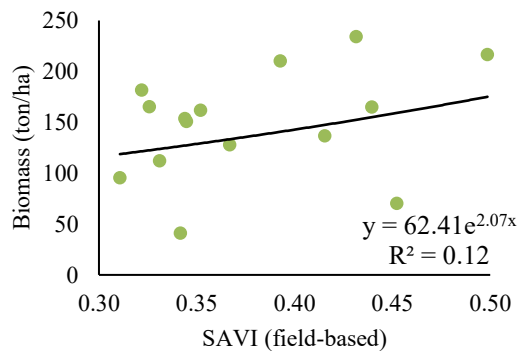


Figure 17: Relationship between field-based SAVI and biomass

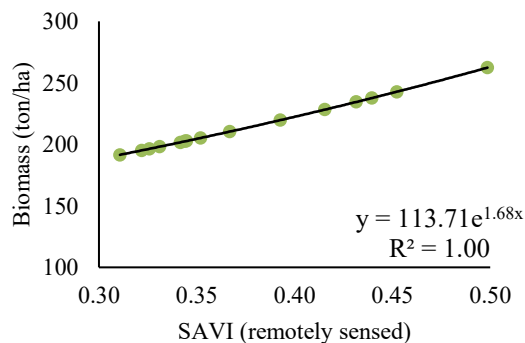


Figure 18: Relationship between remotely sensed SAVI and biomass

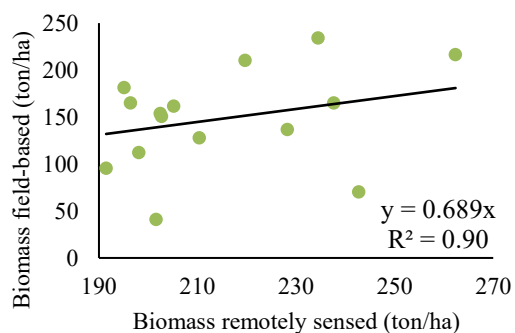


Figure 19: Field-based SAVI and remotely sensed SAVI biomass

Linear regression analysis yielded a coefficient of determination (R^2) of 0.90, indicating that 90% of the variation in field-measured biomass could be explained by satellite-derived SAVI estimates. This strong performance highlights the robustness of SAVI as an alternative vegetation index for improving biomass and carbon stock assessments in heterogeneous urban environments.

3.5 Urban Carbon Stocks

The relationship between field-measured biomass and satellite-derived vegetation indices from Sentinel-2A is presented in Table 2. All tested vegetation indices exhibited coefficients of determination (R^2) greater than 0.90, confirming the strong capacity of Sentinel-2A imagery to capture biomass variability in urban ecosystems. Among these indices, the Normalized Difference Vegetation Index (NDVI) achieved the highest accuracy ($R^2 = 0.91$), thereby selected as the most reliable indicator for estimating biomass and carbon stocks in Malang City. This superior performance can be attributed to NDVI's ability to effectively represent vegetation greenness and canopy cover, which are the primary components of carbon sequestration.

Table 1: Relationship between field-based and remotely sensed biomass

Vegetation Index	Regression Equation	R^2
NDVI	$y = 0.688x$	0.91
EVI	$y = 0.611x$	0.90
ARVI	$y = 0.666x$	0.90
SAVI	$y = 0.689x$	0.90

Further emphasized that tree diversity within urban landscapes plays a pivotal role in enhancing carbon storage and ecosystem resilience. Conversely, the Enhanced Vegetation Index (EVI) and the Atmospherically Resistant Vegetation Index (ARVI) slightly underestimated biomass in low-density vegetation due to their higher sensitivity to atmospheric variations and dense canopy structures. Canopy structure and vegetation type strongly affect vegetation index performance. Similarly, the Soil Adjusted Vegetation Index (SAVI), although designed to minimize soil background influence, demonstrated lower predictive power in urban contexts compared to NDVI. Vegetation indices tend to overestimate biomass in sparse vegetation areas, such as shrubs and grasses, as spectral signals from these covers are often misclassified as denser vegetation. Overestimation contributed to avoiding underestimation of carbon stocks [16] and [17]. In urban planning, such bias can be strategically beneficial, as it prevents the underreporting of green

carbon potential and supports climate change mitigation policies in metropolitan regions. Based on NDVI as the best-performing index, the spatial distribution of carbon stocks in Malang City is summarized in Table 3. The total carbon stock reached 3,861.35 ton/ha, with significant inter-district variability.

Table 3: Spatial distribution of carbon stock in the subdistricts of Malang City

Sub-district	Carbon stocks (ton/ha)
Lowokwaru	591.95
Blimbing	968.50
Klojen	940.62
Sukun	630.25
Kedungkandang	730.03
Total	3,861.35

Spatial analysis revealed distinct spatial heterogeneity in carbon stock distribution across Malang City, strongly influenced by land-use intensity, vegetation cover, and the degree of urbanization. Blimbing and Klojen sub-districts, exhibiting carbon densities exceeding 900 ton/ha, correspond to areas with extensive green corridors, mature tree stands, and peri-urban transition zones characterized by relatively intact vegetation structure. In contrast, Lowokwaru and Sukun represent transitional urban–semi-urban landscapes with moderate carbon densities ranging from 600 to 750 ton/ha, while the lowest carbon density occurred in compact urban cores dominated by impervious surfaces and limited green space.

Urban zones with higher vegetation biomass act as critical ecological buffers, regulating microclimate, mitigating urban heat island effects, and sustaining biodiversity within metropolitan ecosystems. The loss or degradation of vegetation within these high-carbon areas could significantly undermine the city's carbon sequestration potential and exacerbate vulnerability to thermal and hydrological stress. Internal ecosystem attributes, particularly stand density and species composition, exert a decisive influence on carbon productivity. Stand density has a stronger quantitative impact on carbon accumulation than species diversity, although both attributes are fundamental to maintaining long-term biomass resilience against urban stressors such as pollution, soil compaction, and elevated temperature [18].

Urban districts with lower carbon stocks therefore require targeted green infrastructure interventions to restore ecological balance. Measures such as vertical greening systems, rooftop gardens, urban forestry corridors, and vegetation-based landscape architecture can substantially enhance

biomass retention within highly built-up environments. These strategies are particularly crucial because the conversion of vegetated surfaces to impervious cover has been shown to increase land surface temperature (LST) and alter urban hydrometeorological patterns in East Java [19]. Integrating vegetation index algorithms into spatial planning frameworks enables continuous monitoring of carbon dynamics and supports evidence-based urban policy development. The incorporation of NDVI-derived carbon mapping into municipal green space inventories and climate adaptation strategies provides a scientific foundation for carbon-smart urban design [20].

Overall, the findings underscore that remote sensing–derived vegetation indices are not merely proxies for biomass estimation but also strategic tools for urban carbon governance. By coupling these indices with socio-spatial datasets, such as land use, building density, and demographic distribution. Urban planners can develop adaptive, data-driven approaches for climate mitigation and ecological restoration. Consequently, the integration of urban carbon stock management with vegetation conservation, climate adaptation, and ecological risk mitigation represents a critical pathway toward sustainable and climate-resilient city development.

4. Conclusion

This study demonstrates that all vegetation indices derived from Sentinel-2A imagery exhibit a strong positive relationship with field-based biomass measurements ($R^2 > 0.90$). Among the tested indices, NDVI proved to be the most reliable ($R^2 = 0.91$) for estimating urban carbon stocks. Spatial estimations revealed heterogeneity of carbon stocks across sub-districts, with lower values (<600 ton/ha) observed in densely built-up areas and higher values (>900 ton/ha) in semi-peri urban zones with extensive vegetation cover. The total urban carbon stock in Malang City was estimated at 3,861.35 ton/ha, with major concentrations found in city parks, forested landscapes, and heritage green corridors. From an academic perspective, these findings reaffirm the superiority of NDVI in capturing biomass variability within complex urban environments, while broadening the understanding that carbon stock mapping is not only relevant in forested ecosystems but also critical in urban settings. Methodologically, this research contributes to the advancement of remote sensing–based carbon estimation models that can be replicated across cities with diverse biophysical conditions. Practically, the results provide a robust scientific basis for formulating sustainable urban development policies, particularly in supporting the achievement of Sustainable

Development Goals (SDG) 11 (Sustainable Cities and Communities) and SDG 13 (Climate Action). Accordingly, urban vegetation should be regarded as a strategic component of climate governance and a key instrument for mitigating climate change in the era of accelerating urbanization.

Acknowledgment

The authors gratefully acknowledge the support of Lembaga Penelitian & Pengabdian Masyarakat (LPPM), Institut Teknologi Nasional (ITN) Malang, which has funded this research. The authors also thank the European Space Agency (ESA) for providing Sentinel-2A imagery, the primary remote sensing dataset used in this study.

References

- [1] IPCC. (2022). *Climate Change 2022: Mitigation of Climate Change. Contribution of Working Group III to the Sixth Assessment Report of the Intergovernmental Panel on Climate Change*. Cambridge University Press, Cambridge, UK. <https://doi.org/10.1017/9781009157926>.
- [2] Pan, Y., Birdsey, R. A., Fang, J., Houghton, R., Kauppi, P. E., Kurz, W. A., Phillips, O. L., Shvidenko, A., Lewis, S. L., Canadell, J. G., Ciais, P., Jackson, R. B., Pacala, S. W., McGuire, A. D., Piao, S., Rautiainen, A., Sitch, S. and Hayes, D., (2011). A Large and Persistent Carbon Sink in the World's Forests. *Science*, Vol. 333(6045), 988–993. <https://doi.org/10.1126/science.1201609>.
- [3] Seto, K. C. and Pandey, B., (2019). Urban Land Use: Central to Building a Sustainable Future. *One Earth*, Vol. 1(2), 168–170. <https://doi.org/10.1016/j.oneear.2019.10.002>.
- [4] United Nations Human Settlements Programme (UN-Habitat). (2020). *World Cities Report 2020: The Value of Sustainable Urbanization*. Nairobi, Kenya: UN-Habitat. <https://doi.org/10.18356/27bc31a5-en>.
- [5] Lillesand, T. M. and Kiefer, R. W., (1994). *Remote Sensing and Image Interpretation (3rd ed.)*. John Wiley & Sons, New York, USA.
- [6] Huete, A. R., Liu, H. Q., Batchily, K. and van Leeuwen, W., (1997). A Comparison of Vegetation Indices Over a Global Set of TM Images for EOS-MODIS. *Remote Sensing of Environment*, Vol. 59, 440–451. [https://doi.org/10.1016/S0034-4257\(96\)00112-5](https://doi.org/10.1016/S0034-4257(96)00112-5).
- [7] Mondino, E. B., Lessio, A. and Gomasasca, M. A., (2016). A Fast Operative Method for NDVI Uncertainty Estimation and Its Role in Vegetation Analysis. *European Journal of Remote Sensing*, Vol. 49(1), 137–156. <https://doi.org/10.5721/EuJRS20164908>.
- [8] Chang, M. E., Zhao, Z. Q., Chang, H. T. and Shu, B., (2021). Urban Green Infrastructure Health Assessment Based on Landsat 8 Remote Sensing and Entropy Landscape Metrics. *European Journal of Remote Sensing*, Vol. 54(1), 417–430. <https://doi.org/10.1080/22797254.2021.1915881>.
- [9] Reid, C. E., Kubzansky, L. D., Li, J., Shmool, J. L. C. and Clougherty, J. E., (2018). It's Not Easy Assessing Greenness: A Comparison of NDVI Datasets and Neighborhood Types and their Associations with Self-Rated Health in New York City. *Health & Place*, Vol. 54, 92–101. <https://doi.org/10.1016/j.healthplace.2018.08.005>.
- [10] Badan Pusat Statistik Kota Malang. (2023). *Kota Malang Dalam Angka 2023 [Malang City in Figures 2023]*. Malang, Indonesia: BPS Kota Malang. Available online: <https://malangkota.bps.go.id>.
- [11] Kementerian Kehutanan Republik Indonesia. (2012). Peraturan Menteri Kehutanan Republik Indonesia Nomor P.12/Menhut-II/2012 tentang Perubahan Kedua atas Peraturan Menteri Kehutanan Nomor P.32/Menhut-II/2009 tentang Tata Cara Penyusunan Rencana Teknik Rehabilitasi Hutan dan Lahan Daerah Aliran Sungai (RTK RHL-DAS) [Regulation of the Minister of Forestry of the Republic of Indonesia No. P.12/Menhut-II/2012 on the Second Amendment to Forest and Watershed Rehabilitation Technical Planning Procedures]. Jakarta, Indonesia.
- [12] Huete, A. R., (1988). A Soil-Adjusted Vegetation Index (SAVI). *Remote Sensing of Environment*, Vol. 25(3), 295–309. [https://doi.org/10.1016/0034-4257\(88\)90106-X](https://doi.org/10.1016/0034-4257(88)90106-X).
- [13] Badan Standardisasi Nasional. (2011). Standar Nasional Indonesia (SNI) 7724: Pengukuran dan Penghitungan Cadangan Karbon [Ground Based Forest Carbon Accounting]. Jakarta, Indonesia: BSN.
- [14] Mardiatmoko, G., Pietersz, J. H. and Boreel, A., (2014). Ilmu Ukur Kayu dan Inventarisasi Hutan [Timber Measurement and Forest Inventory]. Ambon, Indonesia: Badan Penerbit Fakultas Pertanian Universitas Pattimura.

- [15] Rahayu, S., Lusiana, B. and van Noordwijk, M., (2007). Pendugaan Cadangan Karbon di Atas Permukaan Tanah pada Berbagai Sistem Penggunaan Lahan di Kabupaten Nunukan, Kalimantan Timur [Estimation of Above-Ground Carbon Stock in Various Land-Use Systems in Nunukan Regency, East Kalimantan]. Bogor, Indonesia: World Agroforestry Centre (ICRAF).
- [16] Negassa, M. K., Haile, M., Feyisa, G. L., Wogi, L. and Merga, F., (2025). Modeling and Mapping Spatial Distribution of Baseline Soil Organic Carbon Stock: A Case of West Hararghe, Oromia Regional State, Eastern Ethiopia. *Soil & Tillage Research*. <https://doi.org/10.1080/24749508.2023.2167632>.
- [17] Khamnoi, W., Homhuan, S., Suwanprasit, C., and Shahnawaz. (2024). Assessment of Post-Harvest Rice Crop Biomass and Carbon Stock using Remote Sensing Data in Google Earth Engine. *International Journal of Geoinformatics*, Vol. 20(8), 88–101. <https://doi.org/10.52939/ijg.v20i8.3459>.
- [18] Wirabuana, P. Y. A. P., Setiahari, R., Sadono, R., Lukito, M. and Martono, D. S., (2021). The Influence of Stand Density and Species Diversity on Timber Production and Carbon Stock in Community Forests. *Indonesian Journal of Forestry Research*, Vol. 8(1), 13–22. <https://doi.org/10.20886/ijfr.2021.8.1.13-22>.
- [19] Suharyanto, A., Maulana, A., Suprayogo, D., Devia, Y. P. and Kurniawan, S., (2023). Land Surface Temperature Changes Caused by Land Cover/Land Use Properties and their Impact on Rainfall Characteristics. *Global Journal of Environmental Science and Management*, Vol. 9(3), 353–372. <https://doi.org/10.22034/GJESM.2023.03.05>.
- [20] Andita, A. and Hidayati, N. I., (2025). Assessing CO₂ Absorption of Urban Trees Using NDVI, SAVI, and MSARVI in Salatiga, Indonesia. *International Journal of Geoinformatics*, Vol. 21(4), 18–34. <https://doi.org/10.52939/ijg.v21i4.4063>.